Soil & Tillage Research 215 (2022) 105205

Contents lists available at ScienceDirect

Soil & Tillage Research

journal homepage: www.elsevier.com/locate/still

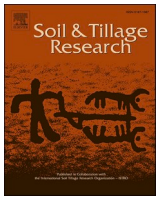

Differences in the sediment composition of wind eroded sandy soils before and after fertilization with poultry manure

Steffen Münch [a,*], Natalie Papke [a], Martin Leue [a], Matthias Faust [b], Kerstin Schepanski [c], Paul Siller [d], Uwe Roesler [d], Ulrich Nübel [e], Tina Kabelitz [f], Thomas Amon [d,f], Roger Funk [a]

[a] Leibniz Centre for Agricultural Landscape Research (ZALF), Eberswalder Str. 84, 15374 Müncheberg, Germany
[b] Leibniz Insitute for Tropospheric Research (TROPOS), Permoserstr. 15, 04318 Leipzig, Germany
[c] Institute of Meteorology, Freie Universität Berlin, Carl-Heinrich-Becker-Weg 6-10, 12165 Berlin, Germany
[d] Insitute for Animal Hygiene and Environmental Health, Freie Universität Berlin, Robert-von-Ostertag-Str. 7–13, 14163 Berlin, Germany
[e] Leibniz Institute DSMZ – German Collection of Microorganisms and Cell Cultures, Inhoffenstr. 7B, 38124 Braunschweig, Germany
[f] Leibniz Institute for Agricultural Engineering and Bioeconomy (ATB), Max-Eyth-Allee 100, 14469 Potsdam, Germany

ARTICLE INFO

Keywords:
Sandy soils
Organic fertilization
Poultry manure
Wind erosion
Dust
Saltation

ABSTRACT

Wind erosion is known to be a gradual process of soil degradation on arable lands. Poultry manure fertilization is a common practice to improve physical, chemical and biological soil properties, and is thus an essential part to maintain soil fertility. Shortly after incorporation, poultry manure and soil particles are loosely adjacent without any bonding. This supposedly affects the susceptibility of soils to wind erosion and influence the physical and chemical composition of the wind-eroded sediment. Wind tunnel experiments were conducted with three wind speeds (8, 11, 14 m s^{-1}) and four sandy soils, each fertilized with poultry manure in a common rate of 6 t ha^{-1}. Incorporation of manure in the soils changed the particulate organic matter (POM) composition resulting in increased median particle diameters, carbon contents and hydrophobicity. Wind erosion caused a preferred release of manure particles already at wind speeds close above the threshold of 7 m s^{-1} with the greatest sorting effects in size, shape, and density of the particles. Thus, wind erosion immediately leads to losses of the added organic material. At higher wind speeds the sediment composition rather corresponds to the entire soil or soil-manure mixtures. Depending on the wind speed and total soil loss, potential manure losses between 101 and 854 kg ha^{-1} were accounted, which are 1.7–14% of the fertilization rate. The results indicate a risk of substantial loss or redistribution of poultry manure by wind erosion immediately after incorporation.

1. Introduction

Wind erosion and associated dust emissions from arable lands are a topic of increasing concern, as the composition and the properties of the released dust causes various environmental problems (Zobeck and Pelt, 2015). The main problem is that wind erosion on agriculture fields is often not noticeable as only the upper millimeters of the topsoil are affected. Thus, large areas of erosion and deposition are difficult to recognize. According to Chepil (1960), up to 40 tons per hectare of soil material can be lost annually without any visible effects. Single wind erosion events caused soil losses of more than hundred tons per hectare, independent of different climatic conditions and land use systems (Fryrear, 1995; Funk et al., 2004; Hoffmann et al., 2011; Michelena and Irurtia, 1995). Climate change will exacerbate the situation, as long lasting droughts and strong winds can be expected in Central Europe during spring and summer (May, 2008; Spinoni et al., 2015; Steininger and Wurbs, 2017). Drier periods have been already determined for the last decades for these seasons in Central Europe (Hänsel et al., 2019; Zolina et al., 2013).

Land use is a further control parameter for wind erosion. Especially summer crops increase the wind erosion risk in spring, as their fields are prepared in the time of the highest erosivity of the year (low precipitation rates and highest mean wind speeds in the spring months) (Borrelli et al., 2015; Funk and Frielinghaus, 1998; Funk and Reuter, 2006; Goossens and Riksen, 2004; Hassenpflug, 1998). Between 2000 and 2018, the acreage for maize increased by 63% in Germany (DESTATIS, 2021) and led to more bare arable land areas in spring. Sandy soils are particularly more susceptible to mechanical stress than soils of finer

* Corresponding author.
E-mail address: steffen.muench@zalf.de (S. Münch).

https://doi.org/10.1016/j.still.2021.105205
Received 6 May 2021; Received in revised form 10 September 2021; Accepted 20 September 2021
Available online 13 October 2021

textures (Lyles, 1985; Zobeck and Pelt, 2015). Tillage at low soil moisture can destabilize the structure of sandy soils completely, leaving a pulverized or single grain structure (Chepil and Woodruff, 1963; Stach and Podsiadłowski, 2002).

There is a close relationship between the size of particles and the critical minimum wind speed for the start of particle movement (Bagnold, 1941). It is lowest for the fine sand fraction (200–63 μm) and is increased for finer (< 63 μm) and coarser fractions (> 200 μm) due to particle bonding between fine particles and increased masses of coarser fractions. Based on German sieving standards, particles > 630 μm are considered as non-erodible fraction (nEF) (Neemann, 1991) that is analogous to the fraction > 840 μm as used in US classification schemes (Chepil, 1941).

Wind erosion is also a very effective sorting process of soil material. Particles of the silt and clay fraction are predominantly removed by transport in suspension mode in the atmosphere, whereas the sand fraction remains on the field or is deposited at the field edge (Buschiazzo and Funk, 2015; Buschiazzo and Taylor, 1993; Li et al., 2009; Shahabinejad et al., 2019). Measurements of wind erosion have also shown enriched carbon contents in the eroded materials (Iturri et al., 2017; Lal, 2003; Li et al., 2018; Nerger et al., 2017; Olson et al., 2016). This is expressed by enrichment ratios (ER) of soil organic carbon (SOC), i.e., the SOC content in the wind-eroded sediment compared to that of the parent soil (Sterk et al., 1996). Sandy soils generally have a higher ER than finer textured soils, indicating an easier separation of organic and mineral components. Independent from the soil type, ER's increase with transport height and distance and ranged between 1.05 and 41.9 (Larney et al., 1998; Li et al., 2009; Sharratt et al., 2018; Webb et al., 2013, 2012). As organic matter and the fine mineral fractions are the carriers of nutrients, wind erosion also results in losses of soil quality (Lei et al., 2019).

Farmyard manure is used to maintain or increase SOC content of soils in order to improve physical, chemical and biological soil properties (Haynes and Naidu, 1998). This is mainly related to the long-term effects. But shortly after incorporation, it is present in the soil as a part of particulate organic matter (POM) and can have an immediate impact on physical soil properties such as water repellency, implicating decreasing infiltration rates or enhanced surface flow and runoff for a certain time (Doerr et al., 2000; Jarvis et al., 2008; McGhie, 1980).

The manure incorporation is concentrated in the top soil layer, i.e. in the tillage horizon. After mixture of manure and soil components, a loose side-by-side of the particles remains for the first period. Depending on soil moisture and microbial activity, different organo-mineral interactions are initiated at different rates. Thus, manure application can lead to a possible combination of two issues. In the long-term, physical soil properties are improved and the risk of soil erosion is reduced due to increased aggregation. In the short-term, susceptibility to wind erosion is temporarily increased by adding fine structured and dry material, i.e. from poultry barns. Specific studies about organic fertilizer losses on sandy soils by wind erosion are lacking to date. The present study focusses on this topic to address this gap from the physical point of view. Sandy soils and poultry manure were used for wind erosion experiments in a wind tunnel, simulating typical spring conditions in Germany, when soils are prepared for summer crops.

2. Material and methods

2.1. Soil and poultry manure samples

Soil samples were taken from the plough horizon of four agricultural fields in the Federal States of Mecklenburg-West Pomerania and Brandenburg (North-Eastern Germany), for which wind erosion is a frequently observed phenomenon. Landscapes are dominated by sandy soils (fluvial and aeolian sediments), which were deposited during the Weichselian glaciation of the Pleistocene ice age. Land use is dominated by arable farming. The northern part of the study region, close to the coastline of the Baltic Sea, is characterized by high wind speeds and higher precipitation rates (annual averages of 4.5–4.8 m s^{-1} and 650–700 mm yr^{-1}). The southern part of the study region has generally lower wind speeds and lower precipitation rates (annual averages of 3.6–3.9 m s^{-1} and 450–550 mm yr^{-1}). The entire region has a lower precipitation rate than the German average of 819 mm (DWD, 2019, 2018, 2021a, 2021b).

The soil samples were used to characterize the grain size distribution by dry sieving and the wet pipette method (DIN ISO 11277, 2002). In addition, subsamples were carefully dry-sieved by hand in order to determine the non-erodible fraction > 630 μm (Funk et al., 2019; Funk and Frielinghaus, 1998; Neemann, 1991). Soil water content (SWC) was measured by the gravimetric method (DIN ISO 11465, 1996). The used soils have sand contents (> 63 μm) of 85–91%, low SOC contents (< 1.8%) (Table 1) and are typical for large parts of wind erosion affected arable lands in the North-Eastern German Lowlands (Funk and Reuter, 2006; Steininger and Wurbs, 2017; UBA, 2011).

Before the wind tunnel experiments, the soils were air-dried at 20–22 °C and 50% relative humidity for several weeks to ensure similar moisture conditions for all soils. Depending on the SOC content, water contents of the air-dried samples were between 0.5% and 1.3%. Large aggregates or stones (> 2 cm) were removed.

Poultry manure was obtained from a chicken breeding farm in the study region. The farm uses conventional management practice, with a high animal population density and a periodic use of antibiotics. Wooden chips and sawdust were used as bedding material. The manure was also air-dried for several weeks, resulting in a remaining water content of 10%, and sieved through a 2 mm mesh. The aim was to achieve the same preconditions for a uniform mixture of poultry manure and soil for the entire time of experiments. This pretreatment can also be seen as a reflection of the meteorological conditions in spring, resulting in a fast surface drying of the upper centimeters of a soil or the soil-manure mixtures.

2.2. Wind tunnel experiments

An open circuit push type wind tunnel was used for wind erosion experiments. Two axial fans generated wind speeds up to 18 m s^{-1} inside the working section. In front of the working section, a wind profile was formed with a straightener section, spikes and variable roughness elements made by LEGO™ bricks. The air intake and exhaust took place on the roof of the hall in a height of about 10 m. The working section of the wind tunnel has a length of 6.5 m, a width of 0.7 m and a height of 0.7 m. The floor of the working section was filled with soil material with a depth of 5 cm.

Both transport modes of wind erosion, saltation and suspension, can be measured separately at the end of the working section. A 0.05 m wide and 0.3 m high saltation trap collected and separated the saltation transport in five height segments (0–1 cm, 4–5 cm, 9–10 cm, 19–20 cm, 29–30 cm). During the run, the collected material from the two lowest segments was weighed every 2 s on scales, which were connected to a data logger. An exemplary illustration of the recorded discharge of soil material is depicted in Fig. S1a. The material from the heights of 9–10 cm, 19–20 cm and 29–30 cm was also sampled and weighed in total after each run. The values were used to calculate the total soil losses by regression analysis:

$$q(z) = \quad q_0 e^{-bz} \tag{1}$$

Where $q(z)$ is the transported material [g] with height z [cm], q_0 is the transported material [g] near the surface (0–1 cm) and b is the slope or the measure of the vertical concentration gradient.

Particles < 32 μm and transported in suspension were measured with one Environmental Dust Monitor (EDM 164, GRIMM Aerosol Technique, hereinafter EDM) in the vertical outlet tube of the chamber behind the working section. The EDM measures the number concentration [L^{-1}]

Table 1
Overview of the investigated soil locations and their basic properties.

Site name	Code	Longitude Latitude	Texture class	Sand [%] c/m/f[b]	Silt [%] c/m/f[b]	Clay [%][b]	> 630 µm [%]	SOC [%]	pH ($CaCl_2$)	SWC [%][c]
Gottesgabe	GG	14°11′39″ 52°39′03″	Loamy sand	87 3/30/54	7 5/1/1	6	12.2 11.1[d]	1.3	7	0.9
Klockenhagen	KH	12°23′15″ 54°14′15"	Sand	92 2/19/71	7 3/1/3	1	10.5 7.2[d]	0.9	6.3	0.6
Kuhstorf	KT	11°18′00″ 53°22′46″	Sand	92 2/46/44	7 3/2/2	1	16 16[d]	0.6	5	0.5
Paulinenaue[a]	PA	12°43′10″ 52°41′04″	Sand	92 0/12/80	7 4/2/1	1	69.8 32.4/ 9.8[d]	1.8	4.5	1.3

[a] hydromorphic influenced soil during soil formation.
[b] soil texture: Sand: coarse sand (2000–630 µm)/middle sand (630–200 µm)/fine sand (200–63 µm), Silt: coarse silt (63–20 µm)/middle silt (20–6 µm)/fine silt (6–2 µm) and clay (< 2 µm).
[c] for air-dry conditions in the laboratory: 20–22 °C, 50% relative humidity.
[d] soil samples with poultry manure.

between 0.25 and 32 µm in 6-seconds-intervals and converts the number concentration to mass concentration [µg m^{-3}] (PM_{10}, $PM_{2.5}$, PM_1). More details on the structure and design of the wind tunnel can be found in Funk et al. (2019).

Each experiment consisted of three runs with wind speeds of 8, 11 and 14 m s^{-1}. The wind speed was increased to the target level within 30 s and kept constant for 10 min. During the first run for each soil, wind speed in the wind tunnel was measured with a high precision hot wire anemometer (Lambrecht meteo GmbH, Göttingen, Germany) at four heights above the soil (0.05 m, 0.15 m, 0.30 m, 0.50 m) to calculate the friction velocity u_* from the vertical wind profile. By using u_*, the wind speed is determined at the standard height of 10 m according to standard requirements of the world meteorological organization (WMO, 2018). The wind speeds of 8, 11 and 14 m s^{-1} in the tunnel correspond to 10.7, 14.8 and 18 m s^{-1} at 10 m height.

After the third wind tunnel run with the highest wind speed level, the deposited saltation material was completely collected and weighed for comparison with the calculated soil losses. Before the experiments were repeated with the same soil, the soil surface was turned and refreshed by mixing the eroded soil material with the soil in the working section uniformly with a rake to achieve the original state of the soil. The same procedure has been repeated two times for each soil, resulting in three experiments per soil with same wind speeds.

After finishing the wind erosion experiment with the soils, the same experiments were repeated with soil-manure mixtures. The added poultry manure corresponded to a common fertilization rate of 6 tons per hectare and an incorporation depth of 0.1 m, resulting in a manure amount of 1.4 kg for the whole wind tunnel working section. Poultry manure was evenly distributed with a hand scoop and incorporated by a rake.

Before the first run, soil samples from the soil surface were taken at five different positions along the working section. The samples and the sediments in the saltation trap were used to analyse the carbon- (C_t) and nitrogen (N_t) content, POM quality and particle size. Since the carbon contents were mainly of organic origin (~ 99% SOC), it was sufficient to show the C_t content in the results. The C mass losses per area were calculated by using the mean weighted C_t content over all trap heights for the respective wind speed:

$$M_{C_tL} = \quad M_{SL} * C_t \tag{2}$$

Where M_{CtL} is the area related C loss [kg m^{-2}], M_{SL} is the area related soil loss [kg m^{-2}] and C_t is the dimensionless total carbon content.

By subtracting the area related C loss from soil-manure mixtures and soils, it is possible to determine the total loss of poultry manure through wind erosion.

$$M_{ML} = \frac{M_{C_tML} - M_{C_tL}}{C_{tManure}} \tag{3}$$

Where M_{ML} is the total loss of poultry manure [kg m^{-2}], M_{CtML} is the total area related carbon loss of soil-manure mixtures [kg m^{-2}], M_{CtL} is the total area related C loss of soils [kg m^{-2}] and $C_{tManure}$ is the dimensionless amount of carbon content of poultry manure.

The PM emissions [µg m^{-2}] were determined by summing up the product of the measured PM concentration c [µg m^{-3}] (Fig. S1b) with the air discharge V [m^3] for a complete duration of $t = 10$ min (100 intervals (i) of 6-second-measurements) of each wind speed and dividing through the wind tunnel section area A (4.55 m^2):

$$PM \quad emission = \frac{\sum_{i=1}^{t} c_i * V_i}{A} \tag{4}$$

Analogously to the calculation of total soil loss, the total PM emissions are the sum of all wind speeds.

2.3. Size analysis of primary particles and micro aggregates

The particle and aggregate size analyses for wind erosion studies need a different consideration compared to standard texture analyses as only limited conclusions of the transported grains or aggregates can be drawn from fully dispersed samples. Size analyses of the soils and sediments were carried out with the Malvern Mastersizer 3000 laser diffractometer (Malvern Panalytical ltd, Malvern, United Kingdom) and an automated dry powder dispersion unit (Aero S). The samples pass the measuring unit without any additional dispersion. Each sample was investigated with the same setting to achieve comparable size distributions: *Particle type*: non-spherical, refractive (1.543) and absorption (0.01) index of Quartz, *background-measuring time*: 10 s, *measuring time*: 5 s, *number of runs*: 3 – 10 (depending on the amount of material) and *obscuration range*: 1 – 10% (recommended).

By default the Mastersizer measurement is fundamentally a measurement of the volume distribution (Mastersizer, user manual, 3000, 2015). Therefore, the volume based size distribution of particles and aggregates was used to determine the particle size distribution. The particle size distributions, i.e. median particle diameter d_{p50}, were calculated using the Mastersizer 3000 software (Mastersizer v 3.71, Malvern Panalytical ltd, Malvern, United Kingdom).

2.4. Carbon and nitrogen content and organic matter composition

The total carbon content (C_t) and the nitrogen content (N_t) of the soils and the sediment material in the saltation trap was determined by dry combustion using an elemental analyzer (CNS928-MLC, Leco Instruments GmbH, Mönchengladbach, Germany) (DIN EN 15936, 2012). The measured carbon and nitrogen contents are corrected to “absolutely dry” by multiplying them with a water content factor.

The organic matter composition of the soils and sediment material

was characterized by diffuse reflectance infrared Fourier transform (DRIFT) spectroscopy in the mid-infrared range with respect to its organic functional groups (aliphatic C—H, C═O, C—O—C) (Capriel, 1997; Capriel et al., 1995), using an FTIR spectrometer BioRad FTS 135 (Digilab, Randolph, MA, USA). To avoid micro-topographic effects on DRIFT spectra due to large particle sizes (Leue et al., 2010), the samples were finely ground using a swinging ball mill (Retsch GmbH, Haan, Germany). Spectra were measured between wave number (WN) 4000 and 400 cm^{-1} (wavelengths between 2.5 and 25 μm) by 16 co-added scans at a resolution of 1 cm^{-1}. The spectra were baseline corrected using the Software WIN-IR Pro (Digilab, Randolph, MA, USA) and converted to Kubelka-Munk (KM) units (Kubelka, 1948). The band intensities of C—H groups (WN 2927 and 2858 cm^{-1}) were measured at the vertical distance from a local baseline plotted between tangential points in order to avoid effects of the neighboring O—H band. The summed heights of the C—H bands were used as a parameter for the potential wettability or repellency of organic matter in the samples (Capriel et al., 1995).

2.5. Optical contact angle measurement and drop contour analysis

Droplet contact angles were determined to test soil and soil-manure samples on water repellency, as water repellency can be used as a further indication of wind erosion susceptibility (Doerr et al., 2000). Aliquots of the soil samples were attached on small glass plates, using double-sided adhesive tape (Bachmann et al., 2000). A water drop of 6 μL was set on the material by a thin syringe (dosage needle). In combination with a backlight source, the dissolving behavior of the droplet was recorded with a high-resolution camera (SCA 20, DataPhysics GmbH, Filderstadt, Germany), starting with the moment of the initial contact between droplet and surface. The contact angle (CA) between droplet and soil surface was measured as a function of time (Fér et al., 2016). Its exponential decrease was fitted by a power function:

$$CA = a + bt^{c} \quad (5)$$

Where *CA* is the contact angle [°], *t* is the water droplet deliquescence time [ms], and *a*, *b*, *c* are fitting parameters, which can be used to compare the droplet deliquescence for different samples.

2.6. Statistical analysis

A Mann-Whitney-Test (significance level $*P < 0.05$) was used to examine significant variations in the carbon and nitrogen content, FTIR-signals and particle size values from triplicate samples between the soil-manure mixtures and soil samples. Regression analyses were performed using Origin (OriginPro 9.1.0G, OriginLab Corporation, Northampton, MA, USA).

3. Results

3.1. Wind driven loss of soil, poultry manure and particulate matter (PM_{10}; $PM_{2.5}$)

The wind erosion experiments in the wind tunnel showed a close dependency of the total soil loss on the non-erodible fraction (nEF > 630 μm) for both soil and soil-manure mixtures. They resulted in maximum soil losses of 14.7 kg m^{-2} for the soil with the lowest share of nEF of around 10% and 3.3 kg m^{-2} for the soil with the highest share of nEF of about 70% (Fig. 1a). There is an exponential decrease of soil loss with increasing nEF. The most drastic decrease is shown, if the nEF increased from 5% to 15%. Only small differences of total soil losses could be determined between soils and soil-manure mixtures (GG, KH, KT). While the total soil loss of GG and KH increased from 5 to 6.4 kg m^{-2} and from 14.7 to 15.1 kg m^{-2} after fertilizing with poultry manure, the soil loss of KT decreased from 4.4 to 4.2 kg m^{-2}. The soil loss of PA increased during the runs from 3.3 to 10.1 kg m^{-2} and is caused by a gradual decrease of nEF during the runs (Table 1).

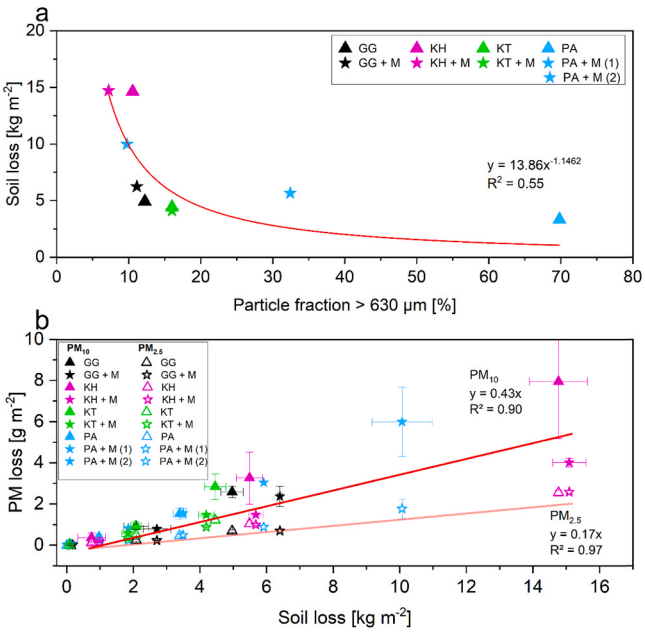

Fig. 1. (a) - Total soil loss in relation of non-erodible particles or aggregates with a diameter > 630 μm after the wind tunnel speed of 14 m s^{-1}, (b) - PM_{10} (solid symbols) and $PM_{2.5}$ (open symbols) losses in relation to the losses of the soils (triangle) and soil-manure mixtures (star) for the wind speeds in the wind tunnel.

The total PM_{10} emissions ranged between 1.5 g m^{-2} and almost 8 g m^{-2}. Total $PM_{2.5}$ emissions ranged between 0.46 and 2.58 g m^{-2}, resulting in a mean $PM_{2.5}/PM_{10}$ ratio of 0.38 ± 0.14. PM_{10} emissions as well as the $PM_{2.5}$ emissions were linear and significantly correlated to the soil losses, whereas the PM_{10} emissions increased more with higher soil losses than the $PM_{2.5}$ emissions (Fig. 1b). Similar to the soil loss results, no differences in PM emissions could be determined between soils and soil-manure mixtures.

Distinct differences between the soils and their mixtures with manure can be seen if the C_t losses are considered (Fig. 2). The relative C_t losses of the soil-manure mixtures are already enhanced at the lowest wind speed of 8 m s^{-1}. If the relative C_t losses are compared, they increase from 3.5% to 8.1% for GG, from 6.8% to 9.5% for KH and from 5% to 13.8% for KT. The next wind speeds (11 and 14 m s^{-1}) yield to similar shares of relative C_t losses for soils and soil-manure mixtures.

The absolute manure losses by wind erosion were calculated from the total soil losses and C_t losses of each experiment and were between 1.7% and 14% of the added amount of manure. This is equivalent to potential manure losses between 101 kg ha^{-1} and 854 kg ha^{-1}, if related to the application amount of 6 tons per hectare (Table 2). On the one hand, the highest relative losses of poultry manure occurred at the lowest wind speed (8 m s^{-1}), where in particular, C was removed (KT, 13.8%). On the other hand, the highest amount of C_t (KH, 854 kg ha^{-1}) gets lost at the highest wind speed (14 m s^{-1}) in correlation to the total soil losses. C_t losses for PA could not be calculated because of an insufficient amount of soil material in the saltation trap at the lowest wind speed.

Soil losses of the maximum wind speed were 19–57 times larger compared to the minimum wind speed, whereas the poultry manure losses were about 3.7 – 6.1 times larger at 14 m s^{-1} compared to 8 m s^{-1}.

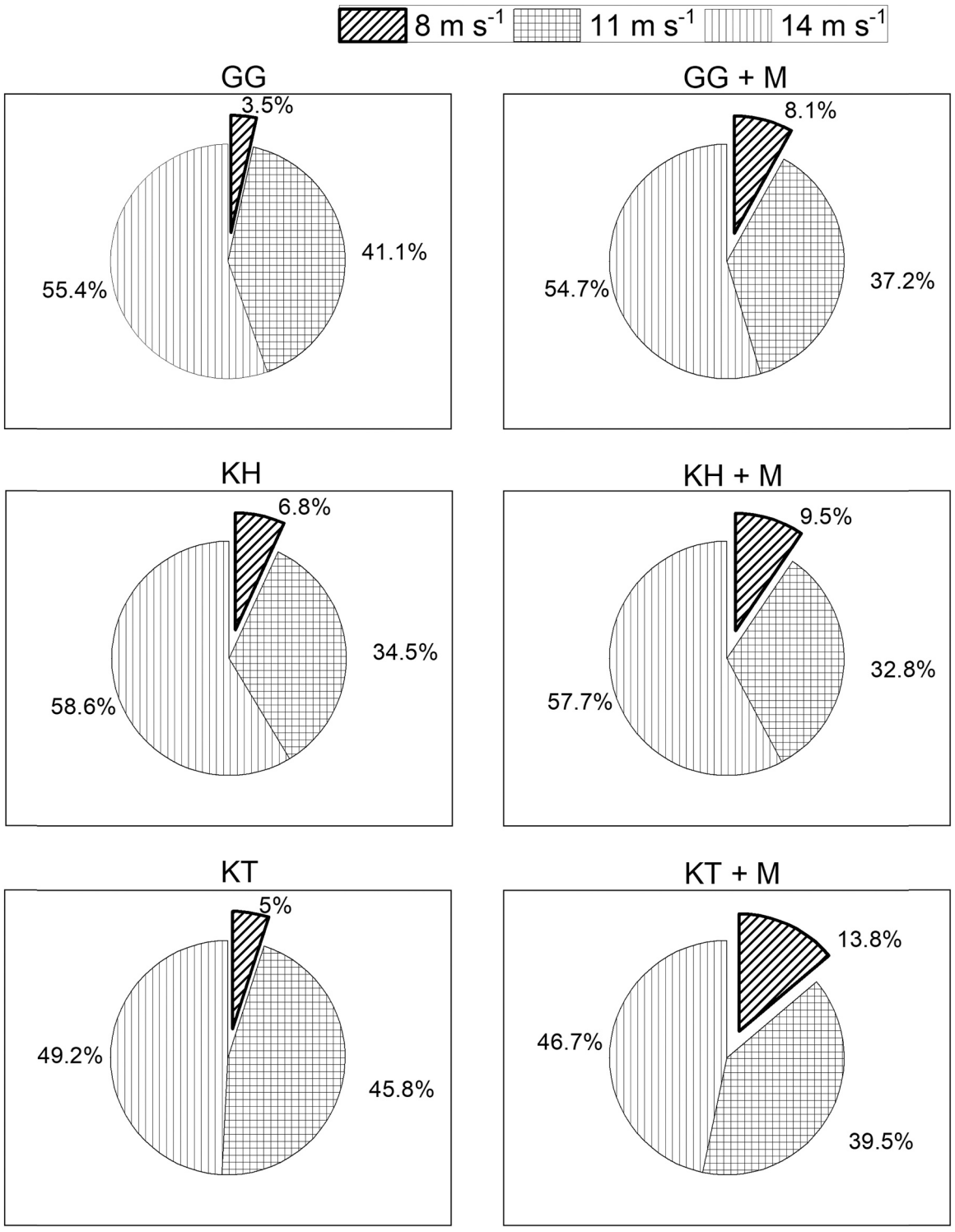

Fig. 2. Percentage of C_t losses in relation to the total C_t loss of the soils (GG, KH, KT) and soil-manure mixtures (GG +M, KH + M, KT+ M) after 14 m s^{-1}.

3.2. Effects of poultry manure on physical and chemical properties of soils and sediments

3.2.1. Soils and poultry manure - particle sizes

The analyses of the samples regarding their non-dispersed grain and/or aggregate size distributions show significant differences between the soils, soil-manure mixtures and the manure (Fig. 3). The manure had a much coarser particle structure compared to the soils. The median diameter d_{p50} of the soils ranged between 177 and 242 μm, whereas the manure had a much larger d_{p50} between 1200 and 1300 μm. The soil-manure mixtures had d_{p50} between 190 and 290 μm.

3.2.2. Soils and poultry manure – POM composition

The SOC contents of the four soils were between 0.6% (KT) and 1.8% (PA) (Fig. 4 and Table 1). In contrast, the manure had an OC-content of 41%, and a N_t content of 4.2%, resulting in a C/N ratio of about 10:1 and therefore ideal for use as organic fertilizer. Due to the relatively low SOC contents of sandy soils, the OC composition changed in quantity and

Table 2
Potential loss of poultry manure and soil at wind tunnel speeds of 8 m s^{-1} (10.7 m s^{-1}), 11 m s^{-1} (14.8 m s^{-1}) and 14 m s^{-1} (18 m s^{-1}) after a poultry manure incorporation of 6 t ha^{-1}.

Code	(8 m s^{-1}) [kg ha^{-1}]		(11 m s^{-1}) [kg ha^{-1}]		(14 m s^{-1}) [kg ha^{-1}]	
	Manure	Soil	Manure	Soil	Manure	Soil
GG	113	864	273	20,864	577	49,676
KH	140	7 473	381	54,879	854	147,656
KT	101	837	212	20,781	373	44,548
PA	N A[a]		N A[a]		N A[a]	

[a] Collected amount was insufficient and soil aggregates were broken due to low aggregate stability during wind tunnel runs

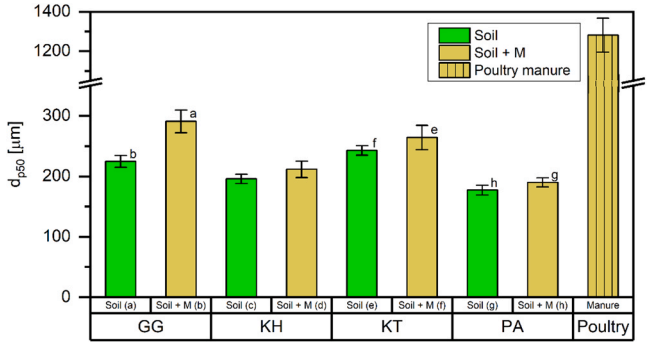

Fig. 3. Median diameter (d_{p50}) of the soil samples (soil, soil-manure mixtures (soil + M) and poultry manure). Please notice the break on the Y-axis. Data are mean values with error bars from triplicate measurements. Letters indicate statistical significance between the differences of soil and soil-manure mixtures of each side.

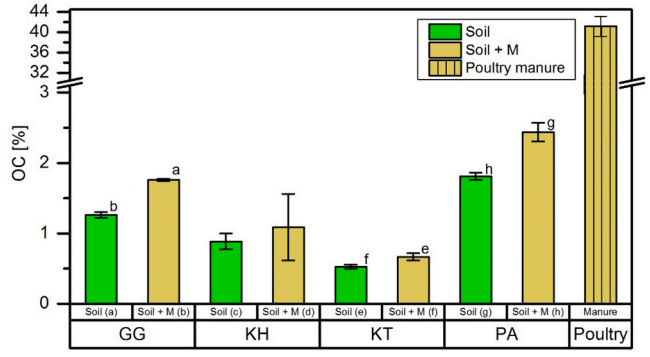

Fig. 4. Organic carbon (OC) contents of the soil samples (soil, soil-manure mixtures (soil + M), and poultry manure). Please notice the break on the Y-axis. Data are mean values with error bars from triplicate measurements. Letters indicate statistical significance between the differences of soil and soil-manure mixtures of each side.

quality when poultry manure of 6 tons per hectare was added to the top layer. Adding poultry manure to the soil resulted in a 1.25-fold increase of SOC for KT and KH and a 1.37-fold increase of OC for GG and PA.

The DRIFT spectra revealed changes in the OM composition after manure application, which can alter the physical and chemical soil properties. In all samples, the signal intensities of C-H groups were higher for the soil-manure mixtures compared to the corresponding soil samples (Fig. 5a), showing factors of 3.4 (KH), 1.9 (KT), 1.5 (GG), and 1.4 (PA).

As the C—H signal intensities of the soil-manure mixtures increased, it should also have an effect on soil wettability (Leue et al., 2015). The contact angles of the droplet decreased more rapidly for soils compared to soil-manure mixtures of all investigated sites (exemplarily shown for GG in Fig. 5b). As well, the initial droplet contact angle on the sample surface of the soil-manure mixture sample (110 ± 7.6°) was higher than for the soil sample (80.4 ± 8°) of GG. Following up, the slope of the contact angles from soil-manure mixtures was flatter than from the soil sample. This can be expressed by the parameter *c* of the power function (Eq. 5), which is a parameter for the curvature of the graph (soil: c = 0.68 ± 0.09; soil-manure mixture: c = 0.45 ± 0.01).

Summarizing the results of all soils, a relatively close relationship was found between the C—H signal intensities, the initial contact angle (R^2 = 0.63, *P < 0.05) (Fig. 5c), the C—H signal intensities and the parameter *c* of the power function (Eq. 5) (R^2 = 0.59, *P < 0.05) (Fig. 5d). Increasing C—H signal intensities were correlated with higher initial contact angles and higher values of the parameter *c* of the power function.

All soils revealed a change in POM composition towards higher OC contents with an increased share of non-decomposed material and increased hydrophobicity after manure application.

3.2.3. Sediments - particle sizes

Fig. 6 shows the particle size compositions of the eroded material in relation to the wind speed and trapping heights. The median diameter d_{p50} of the eroded material varied considerably and increased especially near the surface (0–1 cm) at wind speeds of 8 m s^{-1} compared to the soils without manure. This is a first indication of the higher susceptibility and the preferred transport of particulate organic components by wind erosion. Although easily detached, they remain close to the surface and part of the saltation load. When the soil contains poultry manure, the d_{p50} of the transported sediment increased significantly at the surface from 242 to 306 µm (GG), from 214 to 511 µm (KT), from 162 to 196 µm (KH) and though not significantly, from 151 to 173 µm (PA). The same, but to lesser extent, were detected for the height of 4–5 cm. As the intensity of saltation was weak and friction velocity (u_*) was low at 8 m s^{-1}, no or only a very low amount of material was transported in heights above 5 cm. At the wind speeds of 11 m s^{-1} and 14 m s^{-1}, material was transported and measured at all heights. Here, no clear difference was determined between the d_{p50} of the eroded materials from the soils and soil-manure mixtures. However, for both, the median particle diameter increased with increasing trapping heights. Particle diameters were in the range of 170–200 µm near the surface, and increased to diameters of over 300 µm at the maximum wind speed in the wind tunnel (14 m s^{-1}).

3.2.4. Sediments – POM composition

The ER of C_t in the trapped sediments is a further indication of the origin of the POM. The highest ER's were found in sediments from soil-manure mixtures at the two lowest trap heights and minimum wind speed (Fig. 7). After incorporating poultry manure to the soil bed, the ER of C_t increased differently but significantly for GG from 1.99 to 2.63, for KT from 3.17 to 20.63 and for KH from 0.98 to 1.30. Increasing wind speed and correlated soil losses caused ER's tending to a value of 1, reflecting no further separation, and losses of the entire soils.

The ER for PA could not fully be determined because the traps did not catch enough material at the beginning of the wind tunnel runs due to a high share of aggregates (Table 1). But, because of a general low aggregate stability, a gradual aggregate destruction is visible by greater ER's during the wind tunnel runs for PA. The POM, previously retained in aggregates, was found in the traps at higher wind speeds (11 m s^{-1}, 14 m s^{-1}).

The FTIR signal intensities show the composition of the POM (Fig. 8). The signal intensities of the C—H groups for the eroded sediments of each soil generally increase for the soil-manure mixtures. This concerns mainly the lowest heights at the lowest wind speed (8 m s^{-1}). At 11 and 14 m s^{-1}, increased signal intensities were measured after manure application for all heights. The highest signal intensities in KM were 1.41 for GG at 8 m s^{-1} and 0–1 cm height, 0.7 for KH at 8–11 m s^{-1} and 0–1 cm height, 2 for KT at 8 m s^{-1} and 4–5 cm height and 1.26 for PA at

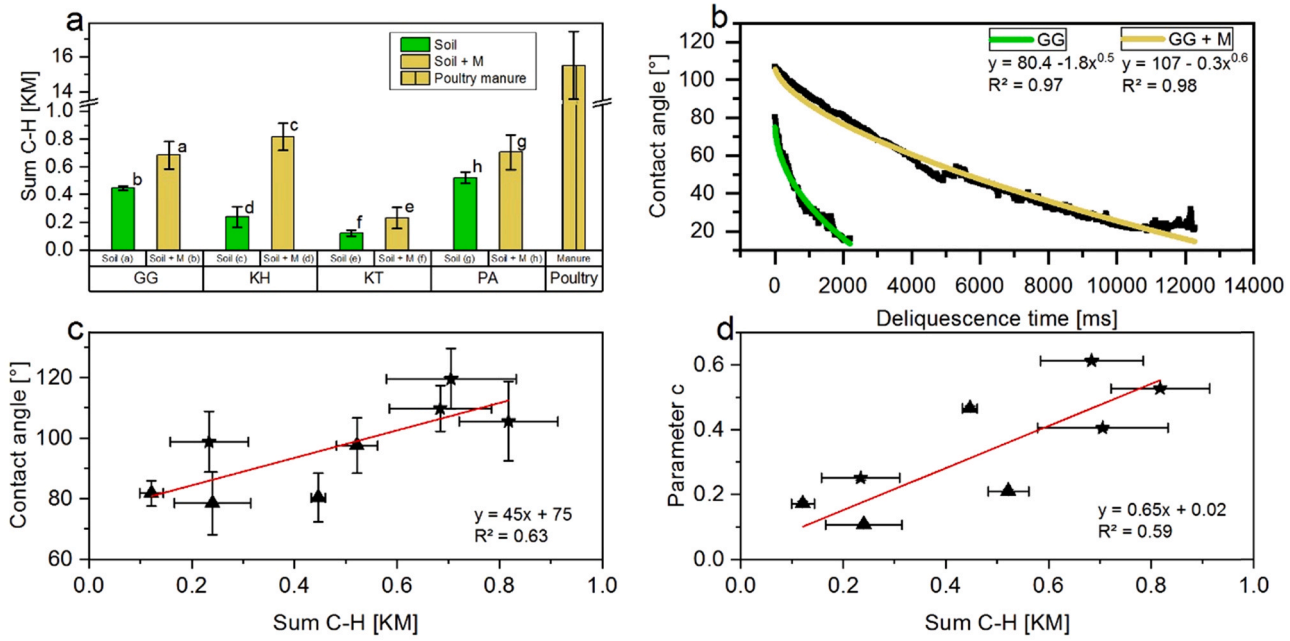

Fig. 5. (a) - FTIR signal intensities of the summed aliphatic C—H groups at WN 2927 and 2858 cm^{-1} of soil samples (soil, soil-manure mixtures (soil +M), and poultry manure) from triplicate measurements, (b) - mean contact angles, exemplary for the soil and soil-manure mixture of GG, (c) – relationship between the signal intensities of the summed aliphatic C—H groups and the first frame of the contact angle and (d) - as well as the parameter c of the power function (Eq. 5). Star symbols in (c) and (d) indicate soil-manure mixtures. Letters in (a) indicate statistical significance between the differences of soil and soil-manure mixtures of each side.

11–14 m s^{-1} and 19–20 cm height. The signal intensity of the C—H groups increased in most of the eroded sediments and show that manure residues were found at almost all heights at each wind speeds. PA is again an exception, since here the higher signal intensities are also due to increasing aggregate decay.

Wind speed depending separation effects between mineral and organic particles are also revealed by the relation of particle sizes (d_{p50}) to the C_t content of the eroded sediments (Fig. 9). There is only a clear linear relationship between increasing d_{p50} and increasing C_t at the lowest wind speed of 8 m s^{-1} (Fig. 9a). This applies to the entire data set (large diagram) as well as to the one cleared of the outlier (small diagram in the upper left corner). R^2 changes only slightly from 0.96 to 0.8. This relationship shows the sorting effects between mineral and organic particles, especially at wind speeds close above the threshold. With increasing wind speeds and soil losses, a correlation could not be determined (Fig. 9b).

Since wind erosion generally leads to a separation between organic and mineral particles, which particularly affects the labile organic matter, it can be further proven via the correlation of the C_t content and the C—H signal intensities. Fig. 10 shows that eroded sediments, independent if fertilized or not, are containing higher amounts of labile organic matter with increasing C_t contents, indicated by higher aliphatic C—H signal intensities. The removal of the outlier improves the correlation between the C—H signal intensities and C_t content (small diagram in the upper left corner). The slightly lower R^2 resulted from the fact that only the second highest signal intensity was measured for the highest C_t content of the sediment load.

4. Discussion

Soils, fertilized with poultry manure, have been identified as a source of fecal bacteria release during wind erosion, being a risk of infections with enterococci (Thiel et al., 2020), *Escherichia coli* (Siller et al., 2021) and *Clostridioides difficile* (Frentrup et al., 2021). The specific properties of poultry manure are a drier consistence and a fine crumbled structure compared to other fertilizers. After manure application and incorporation into soils, a loose side-by-side of organic and mineral particles remains for a certain time if both substrates are relatively dry. Herewith, the manure becomes directly part of the POM of the soil. Application amounts of several tons per hectare can influence physical properties of soils with consequences for wind erosion susceptibility which has not been investigated so far under this focus.

4.1. Potential wind driven loss of soil, poultry manure and particulate matter

Total soil losses, measured in this study in a wind tunnel, were in the range of 3.3–14.7 kg m^{-2} and are comparable to reported soil losses in the literature (Bach, 2008; Funk et al., 2004; Goossens, 2004; Nerger et al., 2017). Differences in absolute soil losses from soils and soil-manure mixtures could not be detected. This is mainly due to the very low density of the manure, which has only a minor influence, as losses are based on the parameter *mass*. Differences between the grain size distributions of soils and soil-manure mixtures could be detected by optical measures and the added manure leads to a general coarser particle structure (Münch et al., 2020). The much lower density of the manure also resulted in only slight changes of the particle size distributions (Table 1), if again based on mass per mesh size after sieving.

Susceptibility of sandy soils to wind erosion is determined by the texture, mainly the non-erodible particle fraction (> 630 μm) as aggregate stability is low. This is in accordance with several wind erosion studies (Chepil, 1960; Funk et al., 2019; Rezaei et al., 2019; Skidmore, 1988; Tatarko, 2001). Three of the soils (GG, KH, KT) were mostly present in the single grain structure, whereas the results of the soil PA show the influence of even weak aggregation. The soil losses of PA increased during the repeated wind tunnel runs, independent if fertilized or not. At the beginning, PA had many aggregates (> 630 μm) resulting from a high soil water content during sampling. Finally, due to a low soil aggregate stability, the aggregates broke by saltation bombardment and repeated mechanical disturbance between the wind tunnel runs, which resulted in gradual increasing losses, finally exceeding the other soils.

The mass share of the added poultry manure, assuming an

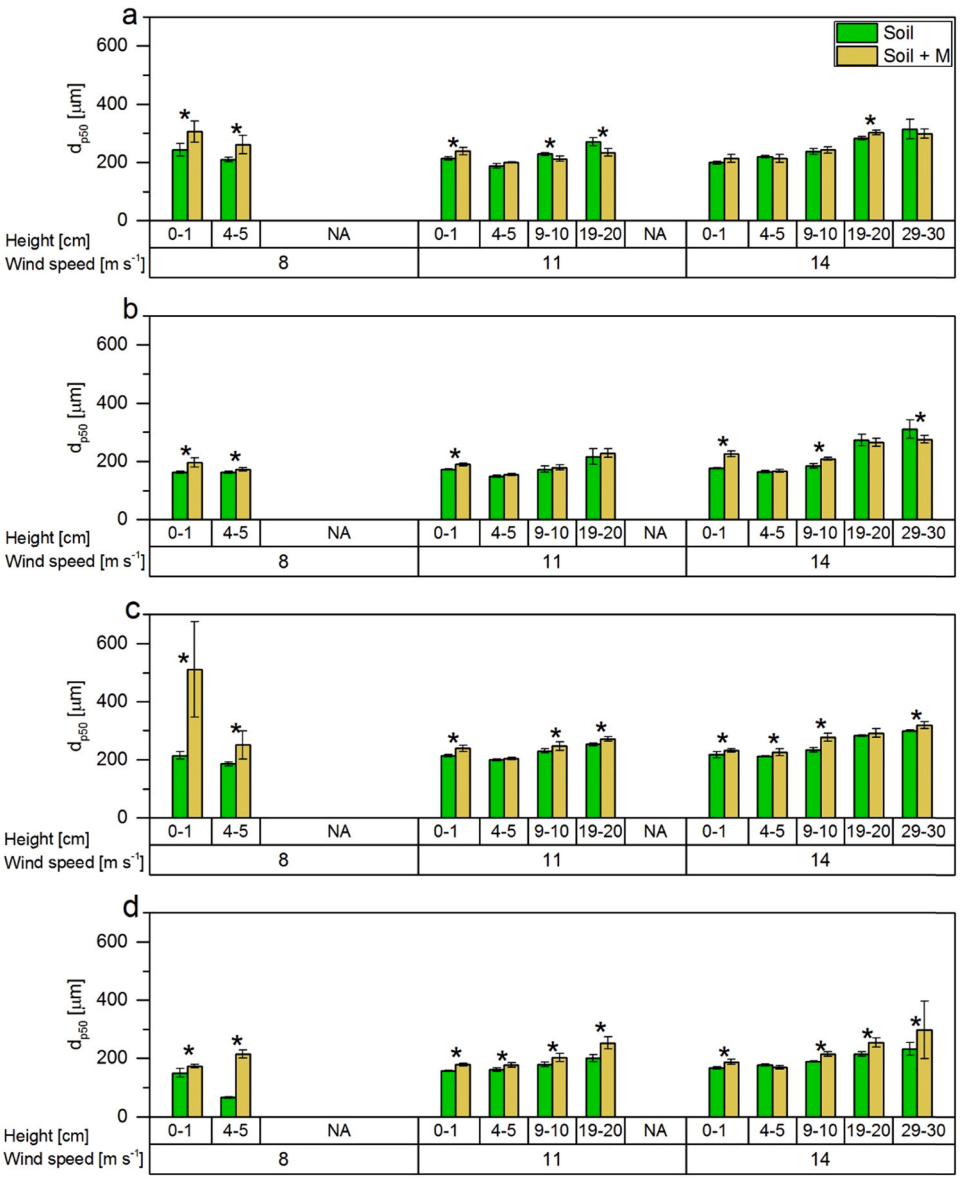

Fig. 6. Median diameter d_{p50} of the trapped sediments of each soil and soil-manure mixtures (soil + M) trapped at the height segments of 0–1, 4–5, 9–10, 19–20 and 29–30 cm at 8, 11 and 14 m s^{-1} in the wind tunnel from (a) GG, (b) KH, (c) KT and (d) PA. Stars indicate significance between soil-manure mixture and soils for each height.

application amount of 6 t ha^{-1} and an incorporation depth of 10 cm, is only 0.4% of the mass of that layer. Based on soil losses and the C_t contents of the sediments, 1.7–14% of poultry manure gets lost by wind erosion. The highest manure losses were measured at the highest wind speed in the wind tunnel, whereas the highest relative losses of manure were determined at the lowest wind speed close above the threshold. Here, the density differences of the organic and mineral particles have the most distinct effect on the beginning of transport, resulting in a preferential release of the organic particles (SOM and manure) from the soil surface. Because of the great differences in u_{*t} for mineral and organic particles it can be assumed, that, once airborne, organic particles are less affected by saturation effects (erosion and deposition in equilibrium) of the saltation transport mode than mineral ones. This is often visible on wind erosion affected fields, where onsite and offsite depositions are characterized by a much lighter color than the original soil (Hassenpflug, 1992). This fact is also confirmed by numerous field studies (Bach, 2008; Larney et al., 1998; Sterk et al., 1996; Webb et al., 2012), where clear correlations were reported between the ER for C_t and the transport height, which can be seen as a proxy for the transport distance. Limitations of the wind tunnel experiments are revealed by the result of the higher wind speeds. A saturation of the transport is not reached in the short measuring section and a separation similar to field lengths of hundreds of meters is not feasible. However, wind speed depending potential losses of a certain area can be derived in a quite easy way.

In contrast to significantly increased dust emissions during the application of dry poultry manure (Kabelitz et al., 2021, 2020; Münch et al., 2020), wind erosion had in this study neither a strengthening nor a reducing effect on the emissions of particulate matter after the incorporation of poultry manure. Similar PM_{10} and $PM_{2.5}$ -emissions were detected between soils and soil-manure mixtures. The total PM emissions, their linear correlation to the soil losses and the ratio of $PM_{2.5}/PM_{10}$ agrees with other wind tunnel studies (Funk et al., 2019; Li et al., 2015; Panebianco et al., 2016).

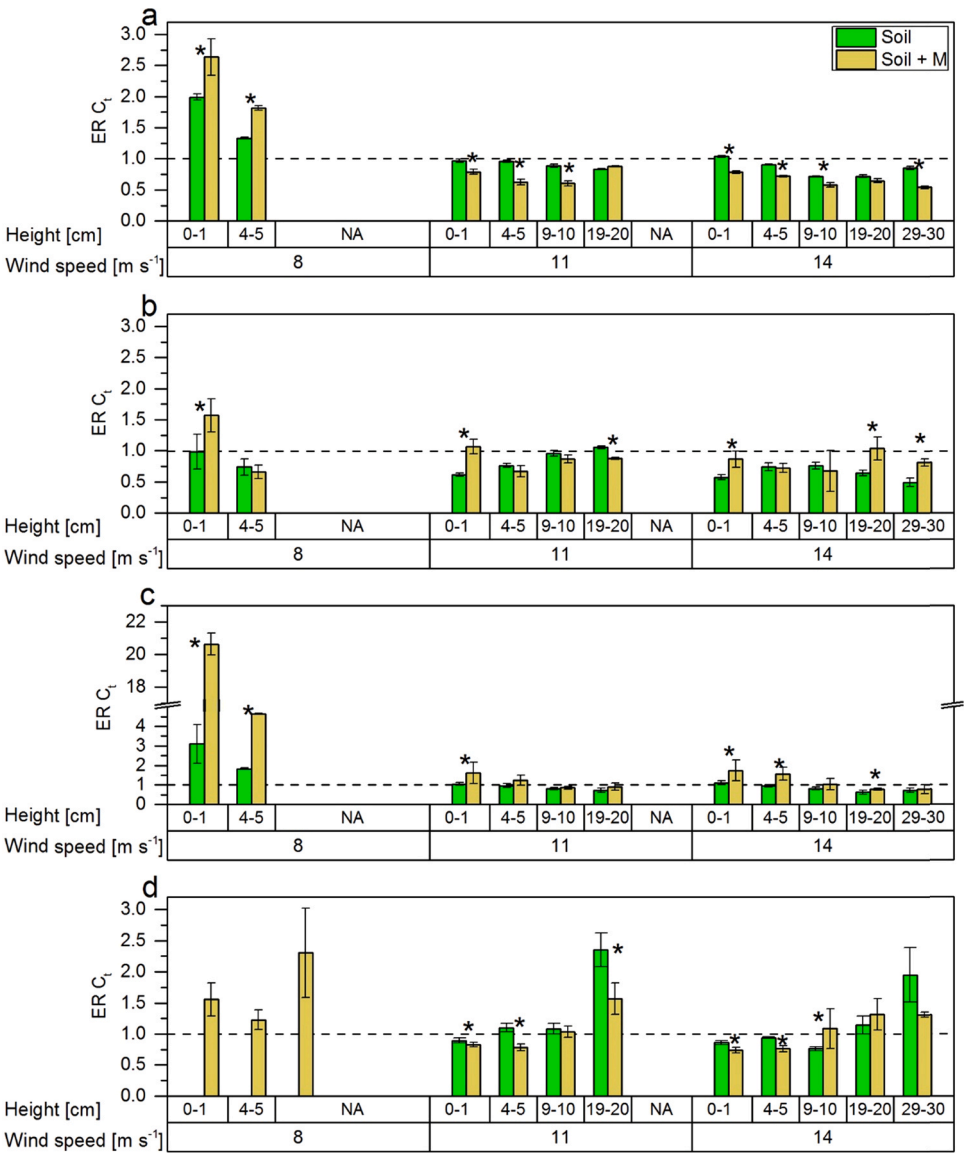

Fig. 7. Carbon (C_t) enrichment ratios (ER's) of the sediments trapped of each soil and soil-manure mixtures (soil + M) at the height segments of 0–1, 4–5, 9–10, 19–20 and 29–30 cm at 8, 11 and 14 m s^{-1} in the wind tunnel from (a) GG, (b) KH, (c) KT and (d) PA. The dotted line indicated the threshold between enrichment (ER > 1) and reduction (ER < 1) of carbon in the sedimentation trap compared to the soil. Stars indicate significance between soil-manure mixture and soils for each height.

4.2. Properties of the investigated soils and sediments before and after adding manure

The added manure leads to increased particle and aggregate sizes in the soil, which has already been reported for short-term by Münch et al. (2020). Due to the low C_t content of the sandy soils, poultry manure fertilization had considerable effects on the momentary C_t contents of all soils (relative increase of 25 – 37%). Because effects of manuring are often considered over the long term, short-term effects are missing from the literature. But long-term monitoring also shows impacts on soil properties by manuring (including poultry manure), such as an increase of mean aggregate diameters and C_t (Agbede et al., 2008; Bhogal et al., 2009; Blanco-Canqui et al., 2005).

Adding manure to the soils changed the composition of POM by increasing the proportion of labile organic compounds, reflected by increased signal intensities of the C—H absorption bands (Iturri et al., 2017). A stronger hydrophobic character was also proven by higher initial contact angles (Leue et al., 2015; Fér et al., 2016). It is widely accepted that soil water repellency is caused by organic compounds derived from living or decomposing plants or microorganisms, when most severe soils are dry (Doerr et al., 2000). The stronger hydrophobicity increases the soil susceptibility to wind erosion, especially for the POM.

In order to initiate wind erosion, a critical threshold value for wind speed or shear stress must first be exceeded. Following Bagnold (1941), the threshold friction velocity u_{*t} is a function of particle diameter and particle density. u_{*t} is lower for particles with a lower density (POM) and increase with increasing particle diameter, whereas the absolute difference of u_{*t} between particles with different densities increase likewise (Fig. S2 Dreisiebner-Lanz and Matzer (2019), Rühlmann et al. (2006)). It shows that the aerodynamic diameter of a poultry manure particle of about 1200 μm (median particle diameter of poultry manure) is the same as for a particle of mineral origin of 250–300 μm. This is the physical reason for the separation of poultry manure particles and mineral particles during wind erosion and becomes particularly obvious at the lowest wind speed above the threshold.

Significant coarser particle compositions were found to be transported near the surface layer resulting in increased ER of C_t. The largest

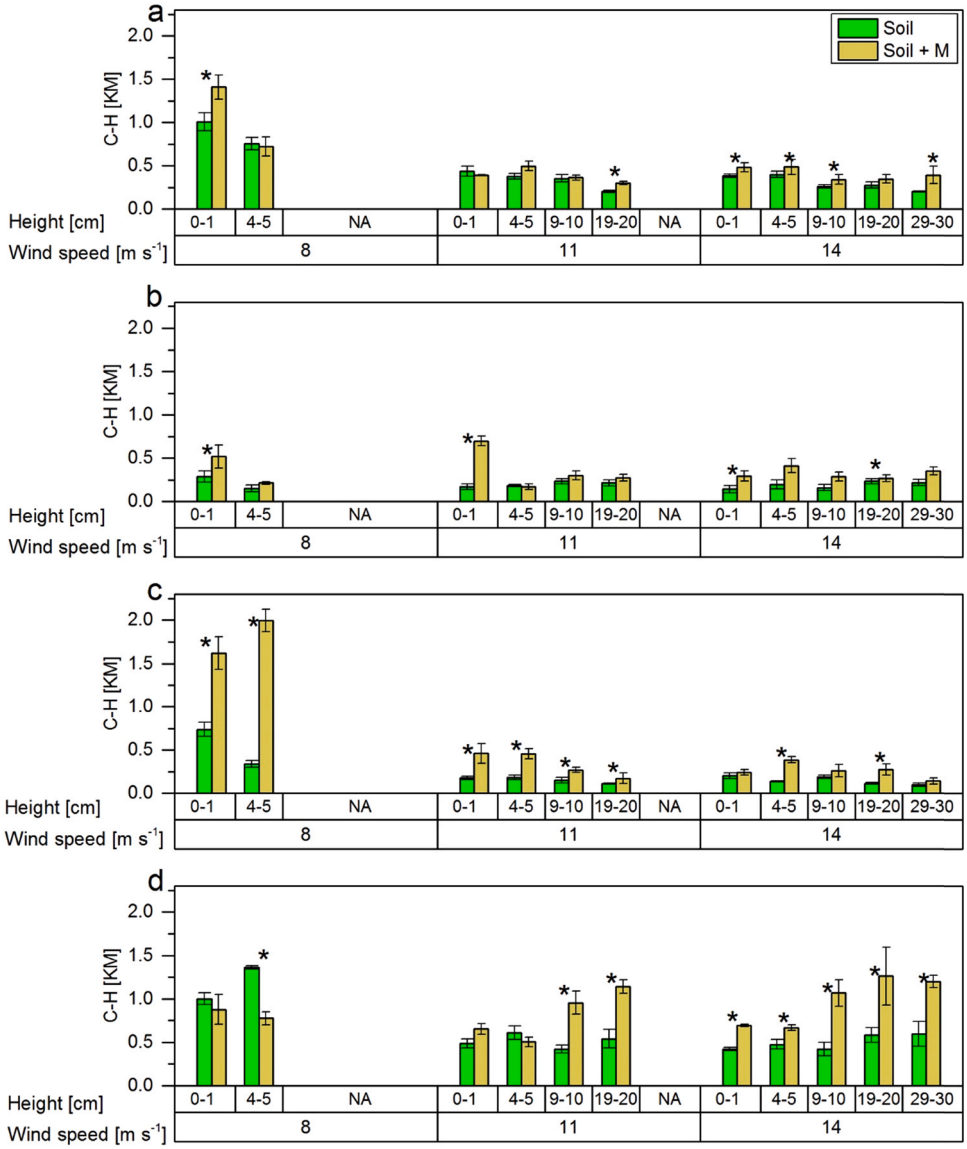

Fig. 8. FTIR signal intensities of the summed aliphatic C—H groups at WN 2927 and 2858 cm^{-1} of the sediments of each soil and soil-manure mixtures (soil + M) trapped at the height segments of 0–1, 4–5, 9–10, 19–20 and 29–30 cm at 8, 11 and 14 m s^{-1} in the wind tunnel from (a) GG, (b) KH, (c) KT and (d) PA. Stars indicate significance between soil-manure mixture and soils for each height.

ER was observed for the soils with the lowest SOC - content (KT) (Fig. 7, Table 1), which is in accordance with Webb et al. (2013). Other studies determined increased ER of C_t also in greater heights because of general higher wind speeds during the experiments (e.g. Iturri et al., 2017). In our study, most of the POM got already lost at the wind speed of 8 m s^{-1}, therefore POM losses at 11 m s^{-1} and 14 m s^{-1} were a corresponding part of the total losses with less separation.

The preferential losses of poultry manure, as a part of POM, were also verified by increased signal intensities of the C—H groups with FTIR analyses. An exception is the soil PA, where the aggregate decay led to a steady resupply of POM in the runs, indicated by higher ER's and C-H signal intensities at higher wind speeds.

4.3. Short-term effects vs. long-term effects of poultry manure on wind erosion

Manure application mitigates land degradation and improves the soil properties due to the addition of organic matter at long-term (Liu et al., 2020). Manuring has several benefits to soil properties, such as improving soil structure, higher water adsorption capacity, enhancing biological activity, soil fertility etc. (Blanco and Lal, 2008).

Manure is applied in a variety of forms, from liquid to solid, in coarse or fine structure. Relevant for wind erosion issues are fine structured, dry manures as poultry manure. Before manure can develop its positive long-term effects, it is incorporated into the soil by mixing tools as cultivators or disc harrows. Depending on the meteorological and soil moisture conditions the soil-manure mixture can be affected first by tillage (Faust et al., 2021) and then by wind erosion shortly after fertilization. As wind erosion is not only a removing but also sorting process, our study provides information of the preferential removal of poultry manure incorporated in sandy soils, depending on the erosion intensity.

Based on this wind tunnel study, it can be concluded that wind erosion may reduce the beneficial effects of poultry manuring. But wind erosion events do not occur every year in mid-latitudes and wind erosion does not necessarily occur directly after fertilization. However, it has already been shown that weather systems, including dry spells, may remain more stationary in mid-latitudes due to climate change (Krüger et al., 2020; Nakamura and Huang, 2018; Stendel et al., 2021). Dry spells decrease the soil moisture and promote the wind erosion risk

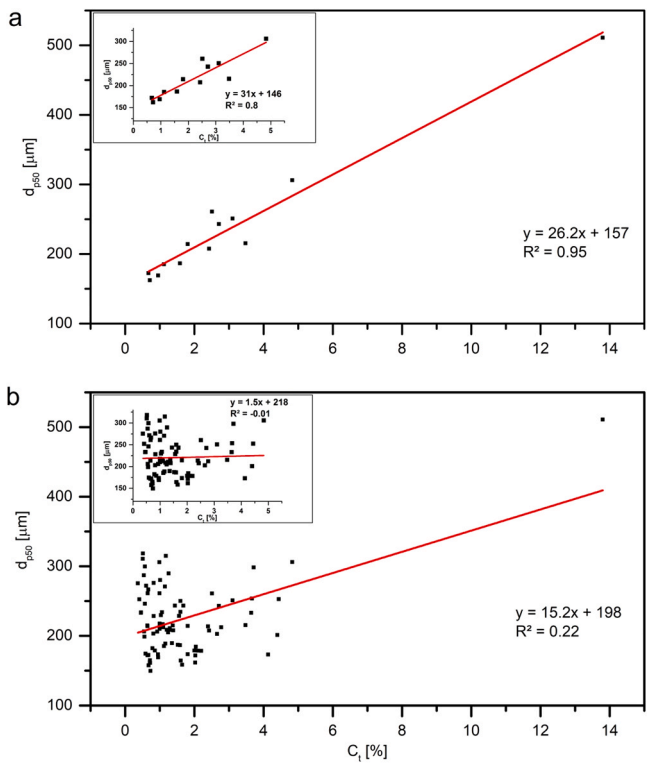

Fig. 9. Mass weighted median particle diameter in relation to C_t from (a) wind tunnel runs at the lowest wind speed (8 m s^{-1}) and from (b) all wind tunnel runs. The small graphics in (a) and (b) showed the relation without the outlier at C_t = 13.8%.

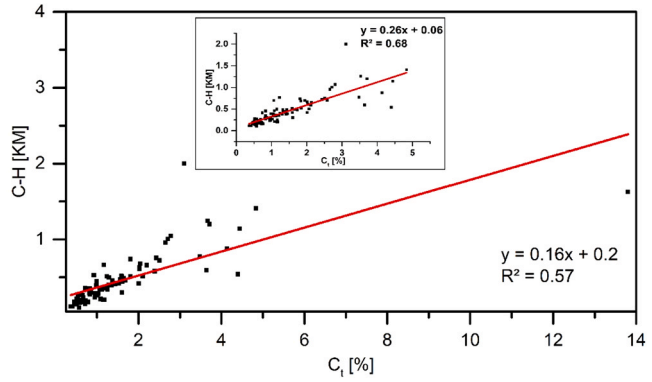

Fig. 10. Mass weighted signal intensities of the summed aliphatic C-H groups at WN 2927 and 2858 cm^{-1} in relation to C_t. The smaller graphic showed the relation without the outlier at C_t = 13.8%.

during high wind intensity, when agricultural fields were fresh tilled.

5. Conclusion

Wind erosion is an effective process of sorting soil particles by size and density removed from sandy arable fields. This also includes freshly incorporated poultry manure. Our wind tunnel experiments showed that the manure particles in sandy soils are additional material for wind erosion. We showed that poultry manure changes physical and chemical properties in the upper soil layer as well as in the wind-eroded sediments. The particularly strong wind events are not decisive in this case. The selective blow-out of the organic fertilizer particles is mainly caused by wind speeds near the wind erosion threshold of 7 m s^{-1}, which occur more frequently (77–86%) than higher wind speeds over the study region in Northeast Germany. Therefore, from the physical point of view, application of a fine structured organic fertilizer, as poultry manure, increases the soil susceptibility to wind erosion. This is particular under the focus, when tillage of dry sandy soil already promotes a single-grain structure. Either the soil or the poultry manure should contain sufficient water to allow binding between the different particles and initiate aggregation.

Declaration of Competing Interest

The authors declare that they have no known competing financial interests or personal relationships that could have appeared to influence the work reported in this paper.

Acknowledgements

The project “Spread of antibiotic resistance in an agrarian landscape” (SOARiAL) was funded by the Leibniz Association, Germany (SAW-2017-DSMZ-2). The authors thank the cooperating poultry farm staff for providing the poultry manure. Many thanks to the reviewers, whose comments helped to improve the manuscript.

Appendix A. Supporting information

Supplementary data associated with this article can be found in the online version at doi:10.1016/j.still.2021.105205.

References

Agbede, T., Ojeniyi, S., Adeyemo, A., 2008. Effect of poultry manure on soil physical and chemical properties, growth and grain yield of sorghum in southwest, Nigeria. Am. -Eurasia J. Sustain. Agric. 2, 72–77.

Bach, M., 2008. Äolische Stofftransporte in Agrarlandschaften: experimentelle Untersuchungen und räumliche Modellierung von Bodenerosionsprozessen durch Wind.

Bachmann, J., Ellies, A., Hartge, K.H., 2000. Development and application of a new sessile drop contact angle method to assess soil water repellency. J. Hydrol. 231–232, 66–75. https://doi.org/10.1016/S0022-1694(00)00184-0.

Bagnold, R.A., 1941. Bagnold, R.A. 1941: the physics of blown sand and desert dunes. London: Methuen. Prog. Phys. Geogr. 18, 91–96. https://doi.org/10.1177/030913339401800105.

Bhogal, A., Nicholson, F.A., Chambers, B.J., 2009. Organic carbon additions: effects on soil bio-physical and physico-chemical properties. Eur. J. Soil Sci. 60, 276–286. https://doi.org/10.1111/j.1365-2389.2008.01105.x.

Blanco-Canqui, H., Lal, R., Owens, L.B., Post, W.M., Izaurralde, R.C., 2005. Strength properties and organic carbon of soils in the North Appalachian Region. Soil Sci. Soc. Am. J. 69, 663–673. https://doi.org/10.2136/sssaj2004.0254.

Blanco, H., Lal, R., 2008. Principles of Soil Conservation and Management. Springer, New York.

Borrelli, P., Panagos, P., Hessel, R., Riksen, M., Stolte, J., 2015. Soil erosion by wind in Europe, EU RECARE Project. pp. 27–38. https://doi.org/10.2788/488050.

Buschiazzo, D.E., Funk, R., 2015. Wind erosion of agricultural soils and the carbon cycle. In: Banwart, S.A., Noellemeyer, E., Milne, E. (Eds.), Soil Carbon: Science, Management and Policy for Multiple Benefits. CABI, Wallingford, pp. 161–168. https://doi.org/10.1079/9781780645322.0161.

Buschiazzo, D.E., Taylor, V., 1993. Efectos de la erosión eólica sobre algunas propiedades de suelos de la Región Semiárida Pampeana Central. Cienc. Suelo 10, 46–53.

Capriel, P., 1997. Hydrophobicity of organic matter in arable soils: influence of management. Eur. J. Soil Sci. 48, 457–462. https://doi.org/10.1111/j.1365-2389.1997.tb00211.x.

Capriel, P., Beck, T., Borchert, H., Gronholz, J., Zachmann, G., 1995. Hydrophobicity of the organic matter in arable soils. Soil Biol. Biochem. 27, 1453–1458. https://doi.org/10.1016/0038-0717(95)00068-P.

Chepil, W.S., 1960. Conversion of relative field erodibility to annual soil loss by wind. Soil Sci. Soc. Am. J. 24, 143–145. https://doi.org/10.2136/sssaj1960.03615995002400020022x.

Chepil, W.S., 1941. Relation of wind erosion to the dry aggregate structure of a soil. Sci. Agric. 21, 488–507. https://doi.org/10.4141/sa-1941-0029.

Chepil, W.S., Woodruff, N.P., 1963. The Physics of Wind Erosion and its Control11Contribution from Soil and Water Conservation Research Division, Agricultural Research Service, USDA, with Kansas Agricultural Experiment Station cooperating. Department of Agronomy Contribution No. 795., in: Norman, A.G. (Ed.), Advances in Agronomy. Academic Press, pp. 211–302. https://doi.org/10.1016/S0065-2113(08)60400-9.

DESTATIS, 2021. Statistisches Bundesamt - Branchen und Unternehmen - Produktionsmethoden - Landwirtschaftliche Betriebe, Fläche: Deutschland, Jahre, Bodennutzungsarten [WWW Document]. Fed. Stat. Off. Wiesb. URL https://www-

genesis.destatis.de/genesis/online?operation=abruftabelleBearbeiten&levelindex=0&levelid=1619353913280&auswahloperation=abruftabelleAuspraegungAuswaehlen&auswahlverzeichnis=ordnungsstruktur&auswahlziel=wertearbruf&code=41141–0001&auswahltext=&werteabruf=Werteabruf#abreadcrumb (accessed 25 May 2021).

DIN EN 15936:2012–11, 2012. Schlamm, behandelter Bioabfall, Boden und Abfall_-Bestimmung des gesamten organischen Kohlenstoffs (TOC) mittels trockener Verbrennung; Deutsche Fassung EN_15936:2012. Beuth Verlag GmbH. https://doi.org/10.31030/1866720.

DIN ISO 11277, 2002. Soil quality - Determination of particle size distribution in mineral soil material - Method by sieving and sedimentation. Ger. Inst. Stand. Dtsch. Inst. Für Norm. EV Beuth Verl. GmbH.

DIN ISO 11465, 1996. DIN ISO 11465 Bodenbeschaffenheit-Bestimmung der Trockensubstanz und des Wassergehaltes auf Grundlage der Masse-Gravimetrisches Verfahren). Beuth Berl.

Doerr, S.H., Shakesby, R.A., Walsh, R.P.D., 2000. Soil water repellency: its causes, characteristics and hydro-geomorphological significance. Earth-Sci. Rev. 51, 33–65. https://doi.org/10.1016/S0012-8252(00)00011-8.

Dreisiebner-Lanz, S., Matzer, R., 2019. Organische Dünger. Fachgr. Tech.

DWD, 2021a. DWD Climate Data Center (CDC): Vieljährige Stationsmittelwerte für die Klimareferenzperiode 1981–2010, für aktuellen Standort und Bezugsstandort, Version V0.x. [WWW Document]. URL https://www.dwd.de/DE/leistungen/cdc/cdc_ueberblick-klimadaten.html (accessed 21 February 2021).

DWD, 2021b. Windkarten und Winddaten für Deutschland Bezugszeitraum 1981 – 2000 [WWW Document]. URL https://www.dwd.de/DE/leistungen/windkarten/deutschland_und_bundeslaender.html# (accessed 21 February 2021).

DWD, 2019. Klimareport Brandenburg. 1 Aufl. Dtsch. Wetterd. Offenb. Am Main Dtschl. 40.

DWD, 2018. Klimareport Mecklemburg-Vorpommern. 1 Aufl. Dtsch. Wetterd. Offenb. Am Main Dtschl. 52.

Faust, M., Wolke, R., Münch, S., Funk, R., Schepanski, K., 2021. A new Lagrangian in-time particle simulation module (Itpas v1) for atmospheric particle dispersion. Geosci. Model Dev. 14, 2205–2220. https://doi.org/10.5194/gmd-14-2205-2021.

Fér, M., Leue, M., Kodešová, R., Gerke, H.H., Ellerbrock, R.H., 2016. Droplet infiltration dynamics and soil wettability related to soil organic matter of soil aggregate coatings and interiors. J. Hydrol. Hydromech. 64, 111–120.

Frentrup, M., Thiel, N., Junker, V., Behrens, W., Münch, S., Siller, P., Kabelitz, T., Faust, M., Indra, A., Baumgartner, S., Schepanski, K., Amon, T., Roesler, U., Funk, R., Nübel, U., 2021. Agricultural fertilization with poultry manure results in persistent environmental contamination with the pathogen Clostridioides difficile. Environ. Microbiol. https://doi.org/10.1111/1462-2920.15601.

Fryrear, D.W., 1995. Soil losses by wind erosion. Soil Sci. Soc. Am. J. 59, 668–672. https://doi.org/10.2136/sssaj1995.03615995005900030005x.

Funk, R., Frielinghaus, M., 1998. Winderosion. In: Handbuch Der Bodenkunde. American Cancer Society, pp. 1–24. https://doi.org/10.1002/9783527678495.hbbk1998003.

Funk, R., Papke, N., Hör, B., 2019. Wind tunnel tests to estimate PM10 and PM2.5-emissions from complex substrates of open-cast strip mines in Germany. Aeolian Res. 39, 23–32. https://doi.org/10.1016/j.aeolia.2019.03.003.

Funk, R., Reuter, H.I., 2006. Wind erosion. In: Soil Erosion in Europe. John Wiley & Sons, Ltd, pp. 563–582. https://doi.org/10.1002/0470859202.ch41.

Funk, R., Skidmore, E.L., Hagen, L.J., 2004. Comparison of wind erosion measurements in Germany with simulated soil losses by WEPS. Environ. Model. Softw. Model. Wind Eros. Aeolian Process. 19, 177–183. https://doi.org/10.1016/S1364-8152(03)00120-8.

Goossens, D., 2004. Wind erosion and tillage as a dust production mechanism on north European farmland. Wind Eros. Dust Dyn. Obs. Simul. Model. ESW Publ. Dep. Environ. Sci. Eros. Soil Water Conserv. Group Wagening. Univ. Wagening. 15–40.

Goossens, D., Riksen, M., 2004. Wind Erosion and Dust Dynamics: Observations, Simulations, Modelling. ESW Publications.

Hänsel, S., Ustrnul, Z., Łupikasza, E., Skalak, P., 2019. Assessing seasonal drought variations and trends over Central Europe. Adv. Water Resour. 127, 53–75. https://doi.org/10.1016/j.advwatres.2019.03.005.

Hassenpflug, W., 1998. Bodenerosion durch wind. Bodenerosion–Analyse Bilanz Eines Umweltprobl. Wiss. Buchgesellschaft Darmstadt 69–82.

Hassenpflug, W., 1992. Winderosion. Handb. Bodenschutzes Kap 2, 200–215.

Haynes, R.J., Naidu, R., 1998. Influence of lime, fertilizer and manure applications on soil organic matter content and soil physical conditions: a review. Nutr. Cycl. Agroecosyst. 51, 123–137. https://doi.org/10.1023/A:1009738307837.

Hoffmann, C., Funk, R., Reiche, M., Li, Y., 2011. Assessment of extreme wind erosion and its impacts in Inner Mongolia, China. Aeolian Res. 3, 343–351. https://doi.org/10.1016/j.aeolia.2011.07.007.

Iturri, L.A., Funk, R., Leue, M., Sommer, M., Buschiazzo, D.E., 2017. Wind sorting affects differently the organo-mineral composition of saltating and particulate materials in contrasting texture agricultural soils. Aeolian Res. 28, 39–49. https://doi.org/10.1016/j.aeolia.2017.07.005.

Jarvis, N., Etana, A., Stagnitti, F., 2008. Water repellency, near-saturated infiltration and preferential solute transport in a macroporous clay soil. Geoderma 143, 223–230. https://doi.org/10.1016/j.geoderma.2007.11.015.

Kabelitz, T., Ammon, C., Funk, R., Münch, S., Biniasch, O., Nübel, U., Thiel, N., Rösler, U., Siller, P., Amon, B., Aarnink, A.J.A., Amon, T., 2020. Functional relationship of particulate matter (PM) emissions, animal species, and moisture content during manure application. Environ. Int. 143, 105577 https://doi.org/10.1016/j.envint.2020.105577.

Kabelitz, T., Biniasch, O., Ammon, C., Nübel, U., Thiel, N., Janke, D., Swaminathan, S., Funk, R., Münch, S., Rösler, U., Siller, P., Amon, B., Aarnink, A.J.A., Amon, T., 2021. Particulate matter emissions during field application of poultry manure - the influence of moisture content and treatment. Sci. Total Environ. 780, 146652 https://doi.org/10.1016/j.scitotenv.2021.146652.

Krüger, J., Pilch Kedzierski, R., Bumke, K., Matthes, K., 2020. Impact of North Atlantic SST and jet stream anomalies on european heat waves. Weather Clim. Dyn. Discuss. 1–21. https://doi.org/10.5194/wcd-2020-32.

Kubelka, P., 1948. New Contributions to the Optics of Intensely Light-Scattering Materials. Part I. JOSA 38, 448–457. https://doi.org/10.1364/JOSA.38.000448.

Lal, R., 2003. Soil erosion and the global carbon budget. Environ. Int. 29, 437–450. https://doi.org/10.1016/S0160-4120(02)00192-7.

Larney, F.J., Bullock, M.S., Janzen, H.H., Ellert, B.H., Olson, E.C.S., 1998. Wind erosion effects on nutrient redistribution and soil productivity. J. Soil Water Conserv. 53, 133–140.

Lei, L., Zhang, K., Zhang, X., Wang, Y.-P., Xia, J., Piao, S., Hui, D., Zhong, M., Ru, J., Zhou, Z., Song, H., Yang, Z., Wang, D., Miao, Y., Yang, F., Liu, B., Zhang, A., Yu, M., Liu, X., Song, Y., Zhu, L., Wan, S., 2019. Plant feedback aggravates soil organic carbon loss associated with wind erosion in Northwest China. J. Geophys. Res. Biogeosci. 124, 825–839. https://doi.org/10.1029/2018JG004804.

Leue, M., Ellerbrock, R.H., Bänninger, D., Gerke, H.H., 2010. Impact of soil microstructure geometry on DRIFT spectra: comparisons with beam trace modeling. Soil Sci. Soc. Am. J. 74, 1976–1986. https://doi.org/10.2136/sssaj2009.0443.

Leue, M., Gerke, H.H., Godow, S.C., 2015. Droplet infiltration and organic matter composition of intact crack and biopore surfaces from clay-illuvial horizons. J. Plant Nutr. Soil Sci. 178, 250–260. https://doi.org/10.1002/jpln.201400209.

Liu, S., Wang, J., Pu, S., Blagodatskaya, E., Kuzyakov, Y., Razavi, B.S., 2020. Impact of manure on soil biochemical properties: a global synthesis. Sci. Total Environ. 745, 141003 https://doi.org/10.1016/j.scitotenv.2020.141003.

Li, P., Liu, L., Wang, J., Wang, Z., Wang, X., Bai, Y., Chen, S., 2018. Wind erosion enhanced by land use changes significantly reduces ecosystem carbon storage and carbon sequestration potentials in semiarid grasslands. Land Degrad. Dev. 29, 3469–3478. https://doi.org/10.1002/ldr.3118.

Li, J., Okin, G.S., Epstein, H.E., 2009. Effects of enhanced wind erosion on surface soil texture and characteristics of windblown sediments. J. Geophys. Res. Biogeosci. 114. https://doi.org/10.1029/2008JG000903.

Li, H., Tatarko, J., Kucharski, M., Dong, Z., 2015. PM2.5 and PM10 emissions from agricultural soils by wind erosion. Aeolian Res., Eight International Conference on Aeolian Research – ICAR 8 19, 171–182. https://doi.org/10.1016/j.aeolia.2015.02.003.

Lyles, L., 1985. Predicting and controlling wind erosion. Agric. Hist. 59, 205–214.

Mastersizer 3000 user manual (English) [WWW Document], 2015. URL https://www.malvernpanalytical.com/en/learn/knowledge-center/user-manuals/MAN0474EN. (accessed 22 October 2019).

May, W., 2008. Potential future changes in the characteristics of daily precipitation in Europe simulated by the HIRHAM regional climate model. Clim. Dyn. 30, 581–603. https://doi.org/10.1007/s00382-007-0309-y.

McGhie, D.A., 1980. The origins of water repellence in some Western Australian soils.

Michelena, R.O., Irurtia, C.B., 1995. Susceptibility of soil to wind erosion in La Pampa province, Argentina. Arid Soil Res. Rehabil. 9, 227–234. https://doi.org/10.1080/15324989509385891.

Münch, S., Papke, N., Thiel, N., Nübel, U., Siller, P., Roesler, U., Biniasch, O., Funk, R., Amon, T., 2020. Effects of farmyard manure application on dust emissions from arable soils. Atmos. Pollut. Res. 11, 1610–1624. https://doi.org/10.1016/j.apr.2020.06.007.

Nakamura, N., Huang, C.S.Y., 2018. Atmospheric blocking as a traffic jam in the jet stream. Science 361, 42–47. https://doi.org/10.1126/science.aat0721.

Neemann, W., 1991. Bestimmung des Bodenerodierbarkeitsfaktors für winderosionsgefährdete Böden Norddeutschlands: ein Beitrag zur Quantifizierung der Bodenverluste; mit 53 Tabellen. Schweizerbart.

Nerger, R., Funk, R., Cordsen, E., Fohrer, N., 2017. Application of a modeling approach to designate soil and soil organic carbon loss to wind erosion on long-term monitoring sites (BDF) in Northern Germany. Aeolian Res. 25, 135–147. https://doi.org/10.1016/j.aeolia.2017.03.006.

Olson, K.R., Al-Kaisi, M., Lal, R., Cihacek, L., 2016. Impact of soil erosion on soil organic carbon stocks. J. Soil Water Conserv. 71, 61A–67A. https://doi.org/10.2489/jswc.71.3.61A.

Panebianco, J.E., Mendez, M.J., Buschiazzo, D.E., 2016. PM10 emission, sandblasting efficiency and vertical entrainment during successive wind-erosion events: a wind-tunnel approach. Bound. Layer Meteorol. 161, 335–353. https://doi.org/10.1007/s10546-016-0172-7.

Rezaei, M., Riksen, M.J.P.M., Sirjani, E., Sameni, A., Geissen, V., 2019. Wind erosion as a driver for transport of light density microplastics. Sci. Total Environ. 669, 273–281. https://doi.org/10.1016/j.scitotenv.2019.02.382.

Rühlmann, J., et al., 2006. A new approach to calculate the particle density of soils considering properties of the soil organic matter and the mineral matrix. Geoderma 130, 272–283. https://doi.org/10.1016/j.geoderma.2005.01.024.

Shahabinejad, N., Mahmoodabadi, M., Jalalian, A., Chavoshi, E., 2019. In situ field measurement of wind erosion and threshold velocity in relation to soil properties in arid and semiarid environments. Environ. Earth Sci. 78, 501. https://doi.org/10.1007/s12665-019-8508-5.

Sharratt, B.S., Kennedy, A.C., Hansen, J.C., Schillinger, W.F., 2018. Soil carbon loss by wind erosion of summer fallow fields in Washington's dryland wheat region. Soil Sci. Soc. Am. J. 82, 1551–1558. https://doi.org/10.2136/sssaj2018.06.0214.

Siller, P., Daehre, K., Rosen, K., Münch, S., Bartel, A., Funk, R., Nübel, U., Amon, T., Roesler, U., 2021. Low airborne tenacity and spread of ESBL-/AmpC-producing Escherichia coli from fertilized soil by wind erosion. Environ. Microbiol. https://doi.org/10.1111/1462-2920.15437.

Skidmore, E., 1988. Wind erosion. Soil Eros. Res. Methods 203–233.

Spinoni, J., Naumann, G., Vogt, J., 2015. Spatial patterns of European droughts under a moderate emission scenario. https://doi.org/10.5194/asr-12–179-2015.
Stach, A., Podsiadłowski, S., 2002. Pulverizing and wind erosion as influenced by spatial variability of soils texture. Quaest. Geogr. 22, 67–78.
Steininger, M., Wurbs, D., 2017. Bundesweite Gefährdung der Böden durch Winderosion und Bewertung der Veränderung infolge des Wandels klimatischer Steuergrößen als Grundlage zur Weiterentwicklung der Vorsorge und Gefahrenabwehr im Bodenschutzrecht. Umweltbundesamt Texte 13/2017, 119.
Stendel, M., Francis, J., White, R., Williams, P.D., Woollings, T., 2021. Chapter 15 - the jet stream and climate change. In: Letcher, T.M. (Ed.), Climate Change, third ed. Elsevier, pp. 327–357. https://doi.org/10.1016/B978-0-12-821575-3.00015-3.
Sterk, G., Herrmann, L., Bationo, A., 1996. Wind-blown nutrient transport and soil productivity changes in southwest Niger. Land Degrad. Dev. 7, 325–335. https://doi.org/10.1002/(SICI)1099-145X(199612)7:4<325::AID-LDR237>3.0.CO;2-Q.
Tatarko, J., 2001. Soil aggregation and wind erosion: processes and measurements. Ann. Arid Zone 40, 251–264.
Thiel, N., Münch, S., Behrens, W., Junker, V., Faust, M., Biniasch, O., Kabelitz, T., Siller, P., Boedeker, C., Schumann, P., Roesler, U., Amon, T., Schepanski, K., Funk, R., Nübel, U., 2020. Airborne bacterial emission fluxes from manure-fertilized agricultural soil. Microb. Biotechnol. 13, 1631–1647. https://doi.org/10.1111/1751-7915.13632.
UBA, 2011. Die Böden Deutschlands. Umweltbundesamt.
Webb, N.P., Chappell, A., Strong, C.L., Marx, S.K., McTainsh, G.H., 2012. The significance of carbon-enriched dust for global carbon accounting. Glob. Change Biol. 18, 3275–3278. https://doi.org/10.1111/j.1365-2486.2012.02780.x.
Webb, N.P., Strong, C.L., Chappell, A., Marx, S.K., McTainsh, G.H., 2013. Soil organic carbon enrichment of dust emissions: magnitude, mechanisms and its implications for the carbon cycle. Earth Surf. Process. Landf. 38, 1662–1671. https://doi.org/10.1002/esp.3404.
WMO, 2018. Guide to Instruments and Methods of Observation, 2018 Edition. ed, WMO. WMO, Geneva.
Zobeck, T.M., Pelt, R.S.V., 2015. Wind erosion. In: Soil Management: Building a Stable Base for Agriculture. John Wiley & Sons Ltd., pp. 209–227. https://doi.org/10.2136/2011.soilmanagement.c14
Zolina, O., Simmer, C., Belyaev, K., Gulev, S.K., Koltermann, P., 2013. Changes in the duration of European wet and dry spells during the last 60 years. J. Clim. 26, 2022–2047. https://doi.org/10.1175/JCLI-D-11-00498.1.